Indian Journal of Biochemistry & Biophysics
Vol. 62, August 2025, pp. 896-908
DOI: 10.56042/ijbb.v62i8.7054

Evaluation of marine algal sulphated polysaccharides as Glucose 6 phosphatase catalytic subunit 1 (G6PC1) inhibitors-A computational approach

Adam S[1], Jayalakshmi A[1], Rajarajan TP[2] & Ranganathan S[1]*

[1]Centre of Biotechnology, Alagappa College of Technology, Anna University, Chennai-600 025, Tamil Nadu, India

[2]Department of Biotechnology, St. Peter's College of Engineering and Technology, Avadi, Chennai-600 054, Tamil Nadu, India

Received 01 December 2023; *revised 10 March 2025*

Glucose 6-phosphatase(G6Pase), an enzyme involved in glycogenolysis and gluconeogenesis, controls glucose production and maintains blood glucose levels through its intrinsic membrane protein, Glucose 6 phosphatase catalytic subunit (G6PC1). G6PC1 inhibition despite being identified as a promising diabetes treatment strategy, effective G6PC1 inhibitors remain unrecognized in the clinical environment. The current investigation concentrates on the computational inhibition of the G6PC1 by marine algal sulphated polysaccharides (SPs). The Ramachandran plot checked the alpha-fold structure of the G6PC1 stereo chemical property through the molprobity server. This study examined 15 SPs for their potent interaction with the G6PC1 enzyme, utilizing a computational approach to identify potent antidiabetic molecules. Among the 15 SPs, drug-likeness, ADMET, and toxicity properties of fucoidan showed promising results that it is nontoxic following the drug-likeness rule. The molecular docking studies signified that fucoidan has the highest binding energy of -4.32 kJ mol^{-1} to the G6PC1 active site compared to other selected SPs. The drug control metformin showed the lowest binding energy of about -3.92 kJ mol^{-1} to the G6PC1. Further molecular dynamics simulations (MD) revealed that the G6PC1-fucoidan complex is stable, as evidenced by the root mean square deviation (RMSD), fluctuations (RMSF) and radius of gyration (Rg) graphs for 50 ns. Overall, data support the potential importance of fucoidan, which could efficiently inhibit or reduce the activity of the G6PC1 enzyme and has proven to be a good measure to control the levels of diabetes in humans; however, further *in vivo* and *in vitro* investigations are required for further validation of these results.

Keywords: Diabetes, Fucoidan, Gluconeogenesis, Glucose homeostasis, Glycogenolysis

Diabetes has emerged as a significant issue within the global population, as highlighted by the International Diabetes Federation Diabetes Atlas. This report indicates that 537 million individuals aged between 20 and 79 years are affected, with projections suggesting an increase to 783 million by 2045[1]. Type 1 (T1DM) and Type 2 diabetes (T2DM) are the two primary forms of diabetes, both characterized by excessive hepatic glucose production(HGP) contributing to hyperglycemia[2]. G6Pase is a multi-component system found in the endoplasmic reticulum that includes transporters for glucose-6-phosphate (G6P), inorganic phosphate, and glucose, as well as a catalytic subunit (G6PC1), among other essential membrane proteins. Hepatocytes receive glucose from circulation, which is phosphorylated by hexokinase IV or glucokinase (GCK), crucial for glucose metabolism and maintaining blood glucose levels within acceptable limits[3]. G6P is hydrolysed back to glucose by G6PC1, which can subsequently be transformed into glucose 1 phosphate (G1P) and uridine diphosphate glucose (UDP-G). Insulin does not directly control glucose uptake; rather, it promotes the conversion of UDP-G to glycogen-by-glycogen synthase, which is then stored in liver cells[4]. The G6PC1 catalyses the reversal reaction that hydrolyses G6P back to glucose, allowing the liver to produce glucose[5]. In other words, hepatic G6P flux is regulated by GCK and G6Pase (G6PC1), which in turn controls blood glucose[6] (Fig. 1). The liver is essential during fasting because it releases glucose into the bloodstream through gluconeogenesis and glycogenolysis[7]. By lowering blood glucose, G6PC1 is a desirable target for the treatment of both T1DM and T2DM. In contrast, G6PC2 inhibition drops blood glucose levels, which may decrease the risk of several ailments, including some types of cancer[8]. Research on various receptors such as human insulin, glucagon-like peptide-1 receptor agonist, biguanides, sulphonylureas, peroxisome proliferator activated receptors, glucose-dependent insulin tropic polypeptide, G-protein coupled receptor 119, free fatty receptor-1, melatonin,

*Correspondence:
E-mail: srenganathan@annauniv.edu; rengsah@rediffmail.com

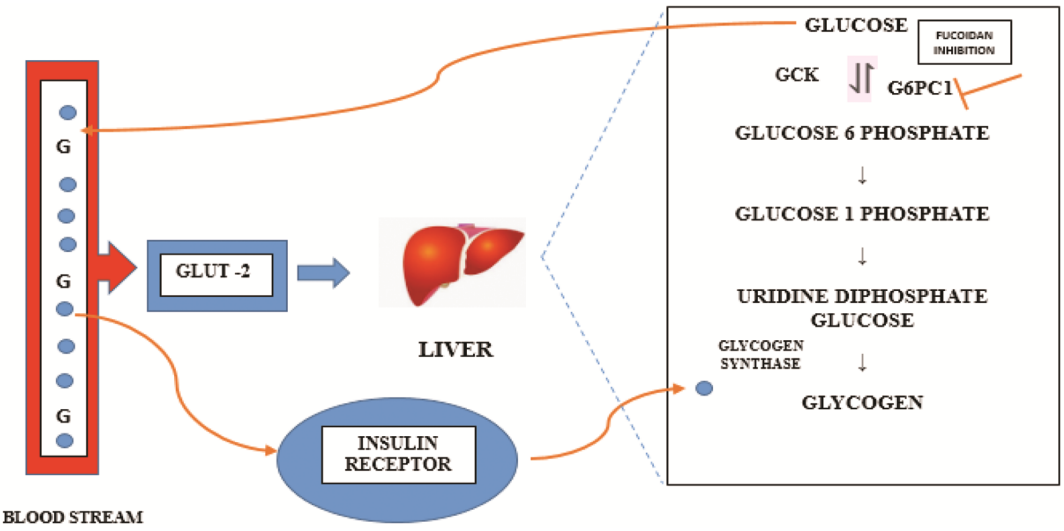

Fig. 1 — Regulation of glucose-G6P cycling in the liver by GCK and G6PC1 and inhibition of G6PC1 by Fucoidan

AMP-activated protein kinase, glycogen synthase kinase-3, protein tyrosine phosphatase 1B, and diacylglycerol acyl transferase has been conducted to control unregulated glucose production. Still, these methods have drawbacks and side effects and can only manage illness and delay complications[9]. Current diabetes mellitus treatments such as metformin, gliptins, sulfonylureas, PPARγ agonists, and α-glucosidase inhibitors also have major limitations and side effects. As a result, there is an ongoing quest to find new pharmacological targets and effective new anti-diabetic drugs. Therefore, inhibiting or reducing the activity of G6PC1 can delay the release of free glucose in the circulation and thus aid in controlling the hyperglycemia correlated with T2DM. Although G6PC1 activity suppression may help the patients control their hepatic glucose production, it is crucial to create partial inhibitors because a total reduction of G6PC1 activity would cause glycogen storage disease (GSD 1a)[8]. The recent studies have identified marine algae Sps like fucoidan, which have anti-diabetic effects and potential pharmaceutical applications such as antifungal, antioxidant, antiviral, anti-inflammatory, or antithrombotic effects due to their ionic nature. In addition, fucoidan also has non-poisonous, bio-resorbable, and biocompatible behaviour permitted by the FDA in the Generally Recognized as Safe (GRAS) category[10]. The novel study aims to identify potential G6PC1 inhibitors by analyzing drug likeliness and ADMET properties of 15 SPs using molecular docking and simulation approaches, to understand their interaction with the enzyme.

Materials and Methods

Physico-chemical properties of G6PC1

The G6PC1 protein sequence(P35575)was exported in FASTA format from Uniprot database, (https://www.uniprot.org)and its physico-chemical properties namely: atomic composition, relative molar mass, isoelectric point (pI), aliphatic (AI) & instability index, the extinction coefficient (EC), and grand average of hydropathy (GRAVY) were calculated using the ExPASy protparam program.(https://web.expasy.org/protparam/)[12].

Multiple sequence alignment & evolutionary tree construction

Protein similarity search for G6PC1 was applied against a non-redundant database using the BLAST P program[13] (https://blast.ncbi.nlm.nih.gov/Blast.cgi). The procured homologous sequences were performed with multiple sequence alignment using clustal omega with default parameters to note the similarity among other G6PC1 proteins[14] and generate an evolutionary tree. Conserved sequences were highlighted and displayed visually.

Protein and ligand preparation

The 3D structure of G6PC1 was obtained from Alpha-fold database[15], energy minimized *via* Swiss PDB viewer, and validated using molprobity server. (http://molprobity.biochem.duke.edu/) Secondary structure prediction for G6PC1 was done using Self-Optimized Prediction Method with Alignment (SOPMA) tool[16]. The Selected SPs' SMILES were acquired from the PubChem database and converted into PDB format using the Open babel server. The

SwissADME server (http://www.swissadme.ch/)[17] was utilized to examine the drug-likeliness of SPs.

ADME and PROTOX toxicity profiling

The PreADMET server (https://preadmet.webservice.bmdrc.org/) was used to predict pharmacokinetic parameters of SPs, including Caco2 permeability, Human Intestinal Absorption (HIA), Plasma Protein Binding (PPB), Blood-Brain Barrier permeability (BBB), P-glycoprotein (P-gp) binding parameter and enzyme metabolic profiles (Phase I & II)[18]. Protox-IIserver (https://tox.charite.de/protox3/) was used to predict the toxicological endpoints (hepatotoxicity, carcinogenicity, immunotoxicity, mutagenicity) and toxicity degree (LD_{50}, mg Kg^{-1}) of the selected SPs[19].

Molecular docking analysis

The auto dock program[20] was applied to view the G6PC1 3D model and add gasteiger charges to the entire protein. The grid area was set to 60 Å × 60 Å × 60 Å with a configuration of 0.408 Å to create the grid parameter file. The XYZ coordinates of the key grid point were set to 64.460.55.020 and 62.510. Docking was executed using the Lamarckian genetic algorithm with 10 runs of iterations, a population size of 150, evaluations set to 25,000,000 and the generation number was 27000 with a default mutation rate (0.02) and crossover rate (0.8). The protein-drug interactions, such as bonded and non-bonded energies among the fucoidans, agar, and control drug metformin against G6PC1 were analyzed by utilizing the biovia discovery studio visualizer.

Molecular dynamics simulation

GROMACS simulation package with the CHARMM36 force field was applied for the G6PC1 and G6PC1-fucoidan complex. Ligand topology was generated by creating point charge (SPC) water in a dodecahedral box with a minimum of 1.0 nm distance between any protein atom and the closest box edge. The system was neutralized with Na^+ ions and energy minimization were done using the steepest descent method (50,000 steps), followed by equilibration *via* isothermal-isochoric (NVT) ensemble and an isothermal-isobaric ensemble (NPT) for 1 ns each. All bonds containing H_2 atoms were restrained using the linear constraint solver code and a 50 ns MD run was executed and structural dynamics (RMSD, RMSF, Rg) were analyzed in the GROMACS package[21]. The graphs were schemed using the Xmgrace tool.

Results and Discussion

Physicochemical properties of G6PC1

The G6PC1 protein in humans typically consists of 357 amino acids and has a relative molecular mass of 40.48 kDa. The pI represents the specific pH value at which the protein has zero net charge. The calculated pI of G6PC1 was found to be 8.72, indicating that it is basic. This study supports previous research indicating that membrane proteins are more basic than non-membrane proteins in bacteria, archaea, and eukaryotes[22]. The instability index provides information on the stability of proteins in both *in vitro* and *vivo* conditions[23]. Proteins with an instability index above 40 are considered unstable, with G6PC1 predicted to be stable at 36.80. The AI is directly related to the quantity and proportion of aliphatic amino acids like alanine (A), valine(V), isoleucine (I), and leucine (L), in a protein. The AI of G6PC1 was found to be 111.88, indicating its thermostable nature[24]. This study supports previous findings that a high AI value indicates protein stability across a wide temperature range. The GRAVY score for a protein is determined by dividing the total hydropathy values of all amino acids by the number of residues in the protein. The GRAVY value of G6PC1 was determined to be 0.474. Proteins with higher negative GRAVY scores are hydrophilic and have good solubility, while those with a GRAVY score over 0.4 are considered hydrophobic and difficult to identify on 2-D gels[25] (Table 1).

Table 2 shows a higher percentage of L (14.3%), V (9.8%), A (5.9%), and I (5.6%) in G6PC1, with 20 positively charged amino acids (A + K) and 25 negatively charged amino acids (D + E). The increased presence of negatively charged residues has significant implications for 3D structure and orientation, especially when combined with transmembrane proteins. The quantity of positively & negatively charged residues and the pI determine subcellular localization, interactions,

Table 1 — Physicochemical properties of G6PC1 by PubChem database

S. No	Uniprot ID	Organism	Length of amino acids	Molecular Weight (kDa)	Isoelectric point (pI)	Instability Index	Solubility Index	Aliphatic Index (AI)	GRAVY	EC @ 280 nm
1	P35575	*Homo sapiens*	357	40.48	8.72	36.80	0.250	111.88	0.474	95715

and solubility[22]. The G6PC1 protein's physical and chemical properties, as well as its amino acid composition, reveal high numbers of leucine-rich repeats, which contribute hydrophobic interactions and conformational stability[26]. In addition, assuming that every pair of cys residues forms a cystine, the extinction coefficient (ECs) of G6PC1 was also determined to be 95715 at 280 nm. The predicted ECs of G6PC1 revealed significant concentrations of tyrosine (Y) and tryptophan(W), while cysteine was found in minimal amounts. From our results, G6PC1 could not be analyzed using UV spectral methods, but the measured EC values will aid in investigating protein-ligand interactions[27]. The SOPMA analysis of the G6PC1 protein reveals that 56.86% of its residues in α-helices formation, 13.17% in extended strands, 2.80% in β turns, and 27.17% in random coils. It is also found an infinitesimal % of β -turn and a higher % of α-helix and random coil, which confirms the G6PC1 stability. G6PC1 lacked other 2^0 structures like the 3_{10} helix, π helix, β bridge, bend region, and ambiguous states. (Table 3) G6PC1's 3D structure was obtained from the alpha fold protein structure database, with a high predicted local distance difference test score (pLDDT)of 92.62, indicating more precise predictions[28] (Fig. 2). Our study also analyzed the distribution of φ(phi) and ψ (psi) angles in the G6PC1 using a Ramachandran plot, revealing a favourable zone with 349 amino acid residues (98.31%), favoured rotamers with 285 residues (96.94%), an outlier zone with 3 residues (0.85%), (Fig. 3) poor rotamers with 1 residue (0. 34%), 1 C-β deviation and 17 bad bonds (Table 4). Rama-Z Score of G6PC1 was found to be 1.00 ± 0.43 indicating that it is suitable structure for molecular docking analysis.

Table 2 — Amino acid composition of G6PC1 by ExPASy Protparam

S. No	Amino acid	Number of Amino acids	Percentage (%)
1	Alanine	21	5.9
2	Arginine	8	2.2
3	Asparagine	10	2.8
4	Aspartic Acid	10	2.8
5	Cysteine	7	2.0
6	Glutamine	15	4.2
7	Glutamic Acid	10	2.8
8	Glycine	22	6.2
9	Histidine	11	3.1
10	Isoleucine	20	5.6
11	Leucine	51	14.3
12	Lysine	17	4.8
13	Methionine	5	1.4
14	Phenyl alanine	25	7.0
15	Proline	16	4.5
16	Serine	30	8.4
17	Threonine	15	4.2
18	Tryptophan	13	3.6
19	Tyrosine	16	4.5
20	Valine	35	9.8
21	Pyrrolysine	0	0
22	Selenocysteine	0	0

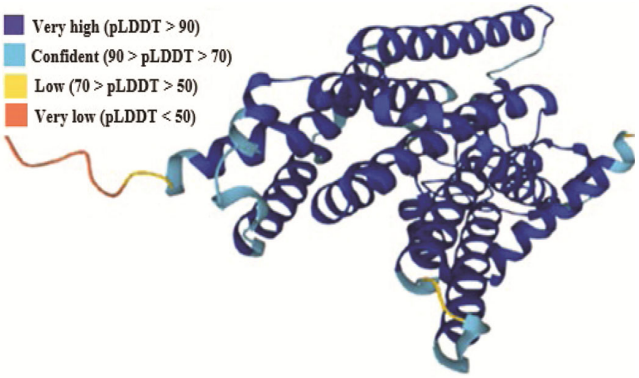

Fig. 2 — 3D Structure of G6PC1 predicted through Alpha fold database

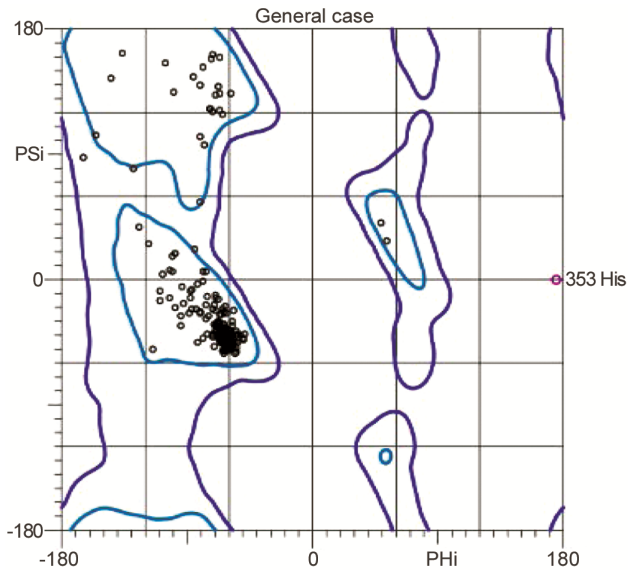

Fig. 3 — Ramachandran plot analysis of G6PC1 using molprobity server

Table 3 — Secondary structure analysis of G6PC1 by SOPMA

G6PC1	α-helix	3_{10} helix	π-helix	β-bridge	Extended strand	β-turn	Bend region	Random coil
No of Amino acid	203	0	0	0	47	10	0	97
%	56.86	0	0	0	13.17	2.80	0	27.17

Table 4 — Ramachandran plot analysis of G6PC1 using mol probity server

	Particulars	Values	Percentage	Reference range
Proteins summary	Poor rotamers	1	0.34%	<0.3%
	Favoured rotamers	285	96.94%	>98%
	Ramachandran outliers	3	0.85%	<0.05%
	Ramachandran favoured	349	98.31%	>98%
	Rama distribution Z-score	1.00 ± 0.43		abs (Z score) < 2
	Cβ deviations >0.25Å	1	0.30%	0
	Bad bonds:	17 / 2964	0.57%	0%

Table 5 — Sequence identity and similarity between G6PC1 using BLAST P

S. No	Name	Query coverage (%)	Identity (%)	Total score	Accession No
1	glucose-6-phosphatase, catalytic (glycogen storage disease type I, von Gierke disease), isoform CRA_a [*Homo sapiens*]	100%	100	727	EAW60901.1
2	glucose-6-phosphatase catalytic subunit 1 isoform 1 [*Homo sapiens*]	100%	100	727	NP_000142.2
3	glucose-6-phosphatase catalytic subunit 1 isoform X1 *[Gorilla gorilla*]	100%	99.44	726	XP_018884157.1
4	glucose-6-phosphatase [*Homo sapiens*]	100%	99.72	726	AAA16222.1
5	G6PC [synthetic construct]	100%	99.72	725	AKI72079.1
6	glucose-6-phosphatase catalytic subunit 1 isoform X1 [*Pan paniscus*]	100%	99.44	724	XP_003813967.3
7	G6PC [synthetic construct]	100%	99.72	724	AKI72078.1
8	G6PC isoform 1 [Pan troglodytes]	100%	99.44	724	PNI33760.1
9	G6PC [synthetic construct]	100%	99.72	724	AKI72077.1
10	G6PC [synthetic construct]	100%	99.72	723	AKI72076.1
11	glucose-6-phosphatase catalytic subunit 1 isoform X1 [*Pongo abelii*]	100%	98.04	719	XP_024091006.2
12	glucose-6-phosphatase [*Nomascusleucogenys*]	100%	97.76	717	XP_003279539.1
13	G6PC isoform 1 [*Pongo abelii*]	100%	97.76	717	PNJ07010.1
14	glucose-6-phosphatase catalytic subunit 1 [*Hylobates moloch*]	100%	97.76	717	XP_032018516.2
15	glucose-6-phosphatase [*Macaca mulatta*]	100%	98.04	716	XP_001112333.2
16	glucose-6-phosphatase [*Macaca nemestrina*]	100%	97.76	716	XP_011723334.1
17	PREDICTED: glucose-6-phosphatase [*Macaca fascicularis*]	100%	97.76	715	XP_005584372.1
18	glucose-6-phosphatase isoform X1 [*Trachipterus francoisi*]	100%	97.76	715	XP_033038779.1
19	glucose-6-phosphatase isoform X1 [*Rhinopithecus roxellana*]	100%	97.76	715	XP_010384053.1
20	PREDICTED: glucose-6-phosphatase [*Mandrillus leucophaeus*]	100%	98.04	715	XP_011854147.1

Evolutionary tree construction

The sequence identity in G6PC1 was found to be between 97.76 and 100%, with a 100% query coverage for the top 20 blast proteins using BLASTP[13] (Table 5). The phylogeny tree shows the classification of G6PC1 into 2 main clades using clustal omega with default parameters (Fig. 4). In first clade, *Pongo abelii* G6Pase catalytic subunit 1 isoform XI and G6PC isoform formed the first cluster. G6Pase of *Nomascus leucogenys* and G6Pase catalytic subunit 1 of *Hylobates moloch* formed a second cluster. G6Pase of *Macaca mulatta, fascicularis*, and *nemestrina* formed a third cluster. The fourth cluster of proteins was formed by G6Pase isoform XI of *Trachypithecus francoisi*, G6Pase of *Mandrillus leucophaeus*, and G6Pase isoform XI of *Rhinopithecus roxellana.* In the second clade, the first cluster was formed by G6Pase catalytic subunit 1 isoform XI of Gorilla. The second cluster of proteins is formed by G6Pase catalytic subunit 1 isoform XI of *Pan paniscus* and G6PC isoform 1 of *Pan troglodytes.* Human G6PC1, G6PC synthetic construct, G6Pase, G6Pase catalytic subunit 1 isoform 1, and G6Pase catalytic isoform CRA_a formed the third cluster protein. To further emphasize the relationship of the genus, the sequences that were close neighbours but in separate clades were aligned pairwise. Sequence alignment of the Pongo G6PC1 isoform XI, a member of clade 1, with the clade 3 *Homo sapiens* G6PC1 isoform 1, they showed a 98.04% sequence identity, whereas *Macaca mulatta* G6Pase, a member of clade 2, shared a 98.04% identity with the clade 3 Homo G6PC1 isoform 1. Furthermore, *Gorilla gorilla* G6PC1 isoform X1 shares a closer evolutionary relationship with human G6PC1isoform 1 showed a 99.04% sequence identity. G6PC1 phylogenetic study result was similar to *Cyprinus carpio* G6PC gene family phylogeny reporting that G6PC proteins of common carp have closer evolutionary relationship, and the same subtype members have higher homology

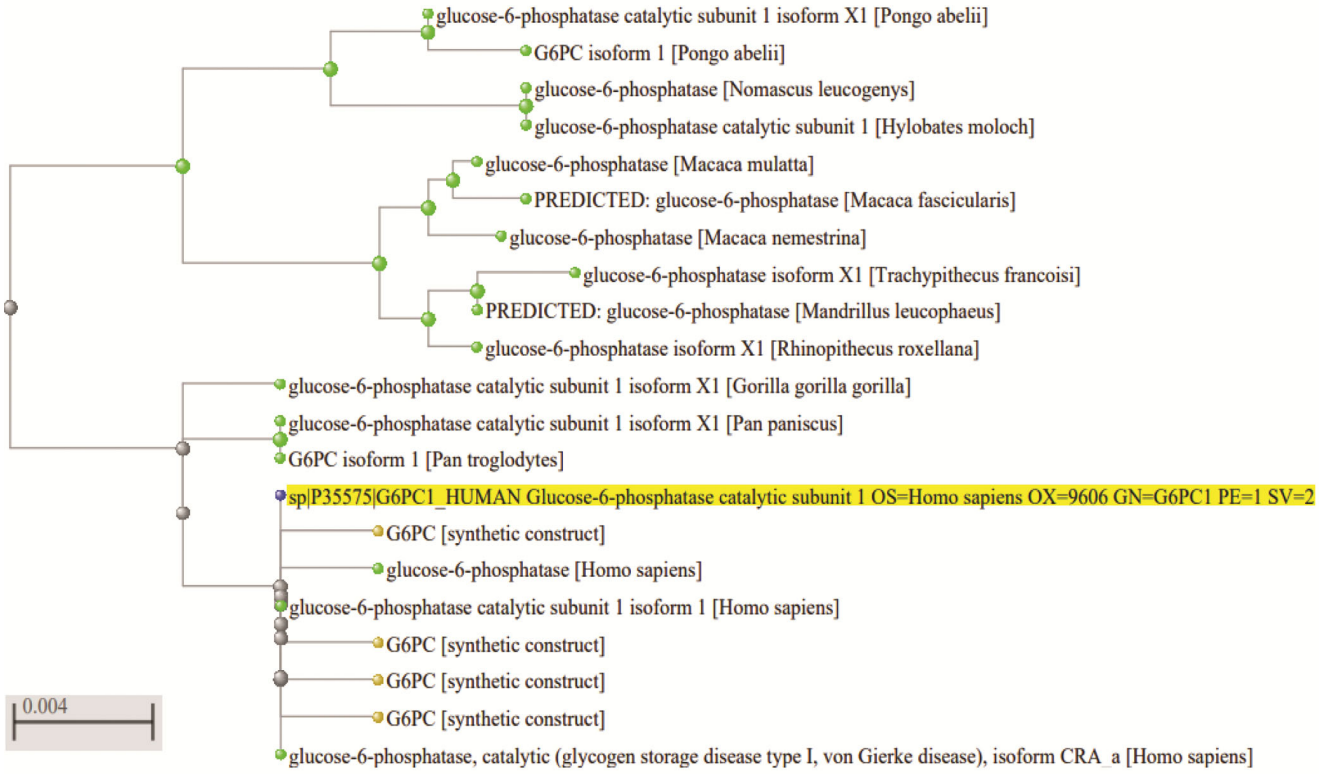

Fig. 4 — Phylogenetic relationship of G6PC1 protein by clustal omega

among different species[29]. Rule of Five (RO5) was used to evaluate the drug-likeness of 15-chosen SPs and metformin, assessing factors like relative molar mass, XLogP3-AA, H_2 bond donor & acceptor count, rotatable bond count, and TPSA. Table 1 show that SP-1 (fucoidan) and SP-2 (agar) meet all RO5 criteria, while most selected SPs do not meet these criteria. Further, our study was carried out using the SPs fucoidan, agar, and the control drug metformin. Octanol-water partition coefficients (XLOGP3-AA) calculate log P in molecules[30], showing fucoidan, agar, and metformin as hydrophilic compounds with -1, -2.2, and -1.3 values, respectively. The TPSA, is an essential and helpful measure for evaluating drug transport characteristics[31], was found to be below 140 $Å^2$ for fucoidan and agar, indicating intermediate intestinal absorption. Finally, rotatable bonds of fucoidan, agar, and metformin were also found to be 3, 4, and 2, respectively. The previous study also indicates that compounds with 10 or fewer rotatable bonds, TPSA of 140 $Å^2$, and 12 or fewer H_2-bond donors and acceptors are likely to have high oral bioavailability in rats[32]. The bioavailability scores for fucoidan and agar showed good absorption after oral administration, with a score of 0.56 and 0.55, respectively[33]. The SwissADME part provides access to 5 rule-based filters (RO5, Ghose, Veber, Egan, and Muegge) with varying attributes for identifying a drug-like molecule. Thus, fucoidan and agar were chosen for further molecular docking studies due to their compliance with all rule-based filters.The pubchem database does not currently contain properties for certain SPs like iota carrageenan, furcellaran, ulvan, rhamnan sulfate, and floridean. Tables 6 and 7 summarizes the drug-likeliness properties, drug rule violations and bioavailability score of selected SPs.

PreADMET assessment of sulphated polysaccharides

The preADMET study revealed that most SPs had pharmacokinetic properties within recommended ranges, except for mannan, λ-carrageenan, K-carrageenan, and porphyran. (Table 8) TheBBB value of fucoidan and agar were less than 2, indicating decreased absorption of Sps to CNS.The HIA value for fucoidan and agar were 58.16 and 32.82, respectively, indicating moderate absorption.PPB, or drug binding to blood proteins, significantly influences drug efficacy[34]. Fucoidan and agar showed weak PPB, with 39.20% and 26.55%, respectively. The predicted absorption value for the Caco2 cell (PCaco2) of fucoidan was found to be

Table 6 — Drug likeliness properties of macroalgal sulphated polysaccharides by pubchem database

S. No	Polysaccharides (Sps)	Pubchem ID	Relative molar mass[a] (g mol^{-1})	XLogP3-AA[b]	H_2 Bond Donor Count[c]	H_2 Bond Acceptor Count[d]	Rotatable Bond Count[e]	TPSA (A^{o2}) [f]
1	Fucoidan	129532628	256.28	-1	2	7	3	110.67
2	Agar	71571511	336.33	-2.2	4	9	4	127.07
3	Galactan	53477780	370.35	-4.2	6	11	6	167.53
4	Alginate	131704328	418.23	-4	6	12	5	219.62
5	Laminarin	439306	504.4	-5.8	11	16	7	268.68
6	Xylan	129539666	574.5	-6	8	17	8	244.91
7	Lambda Carrageenan	91972149	579.5	-6.1	5	20	7	353.27
8	Mannan	25147451	666.6	-9	14	21	10	347.83
9	Kappa Carrageenan	11966249	788.7	-8.5	8	25	10	394.53
10	Porphyran	156595906	852.7	-8.3	10	27	14	434.99
11	Iota Carrageenan	405237818	-	-	-	-	-	-
12	Furcellaran	176259294	-	-	-	-	-	-
13	Ulvan	405234592	-	-	-	-	-	-
14	Rhamnan sulfate	-	-	-	-	-	-	-
15	Floridean starch	-	-	-	-	-	-	-
16	Metformin (Control drug)	4091	129.16	-1.3	3	1	2	91.5

[a]Molecular weight (<500 u). [b]Log of the octanol/water partition coefficient (optimal 0~3; <5); [c]No of hydrogen bond donors (nHD ≤ 5); [d]No of hydrogen bond acceptors (nHA ≤ 10);[e]Rotatablebond count (nRB<10); [f]TotalPolar Surface Area (TPSA ≤ 140A^{o2}).

Table 7 — Drug likeliness rule violations and bioavailability score of macroalgal sulphated polysaccharides by Swiss ADME

		No of violations					
S. No	Polysaccharides	RO5	Ghose	Veber	Egan	Muegge	Bioavailability Score
1	Fucoidan	0	0	0	0	0	0.56
2	Agar	0	1	0	0	1	0.55
3	Galactan	2	1	1	1	4	0.17
4	Alginate	2	1	1	1	4	0.11
5	Laminarin	3	2	1	1	4	0.17
6	Xylan	3	3	1	1	4	0.17
7	Lambda Carrageenan	2	2	1	1	3	0.11
8	Mannan	2	2	1	1	3	0.11
9	Kappa Carrageenan	3	4	2	1	5	0.11
10	Porphyran	3	4	2	1	6	0.11
11	Metformin (Control drug)	0	3	0	0	2	0.55

3.74766, indicating moderately permeable. The fucoidan and agar were identified as non-inhibitors of P-gp. CYP models predict metabolism using substrate or inhibitor categories(CYP1A2, CYP2D6, CYP3A4, CYP2D6, CYP3A4, CYP2C19, and CYP2C9), with 18 families based on amino acid homology, with families 1, 2, and 3 primarily responsible for drug metabolism[35]. The computed metabolism of fucoidan and agar showed inhibitors of CYP_2C19, CYP_2C9, and CYP_3A4 and non-inhibitors of CYP 2D6 inhibition and CYP_2D6 substrate.

PROTOX toxicity profiling

The present study also intended to predict the hepatotoxicity, carcinogenicity, immunotoxicity, mutagenicity, and cytotoxicity of the selected 10 SPs as well as their effects on other organs (Table 9). These findings demonstrate that none of the SPs cause toxic hepatitis, carcinogenicity, or cytotoxicity. Of the investigated SPs, fucoidan shows 1 toxicological endpoint (mutagenicity), and agar shows 1 toxicological endpoint (immunotoxicity). On the other hand, galactan, alginate, laminarin, xylan, λ-carrageenan, mannan, K-carrageenan, and porphyran are not projected to be toxicologically active.

Molecular docking analysis

The molecular docking studies examined the interactions of G6PC1 with selected SPs (fucoidan and agar) and compared the results with the control drug metformin (Table 10 & Fig. 5). As per the prior findings[36], the catalytic core of G6Pase, consisting of amino acids K76, R83, H119, R170, and H176, plays

Table 8 — Pharmacokinetics parameters of the macroalgal sulphated polysaccharides by Pre ADMET server

	Polysaccharides Properties	Fu	Ag	Ga	Al	La	Xy	λ-ca	Ma	K-ca	Po
1	BBB[a]	0.102	0.027	00.32	0.169	0.027	0.058	0.035	0.027	0.036	0.057
2	HIA[b]	58.16	32.82	8.04	4.94	0.099	1.47	0	0	0	0
3	Plasma protein Binding (%)[c]	39.20	26.55	13.60	12.56	5.39	8.93	62.34	4.26	4.40	3.64
4	Caco2[d]	3.74	3.24	4.67	17.47	1.36	8.33	7.55	1.83	0.94	0.83
5	CYP_2C19 Inhibition	In	In	In	In	In	In	In	In	In	In
6	CYP_2C9 Inhibition	In	In	In	In	In	In	In	In	In	In
7	CYP_2D6 Inhibition[e]	NIn	NIn	NIn	Nin	NIn	NIn	NIn	NIn	NIn	NIn
8	CYP_2D6 substrate	NIn	NIn	NIn	Nin	NIn	NIn	NIn	NIn	NIn	NIn
9	CYP_3A4 Inhibition	In	In	In	Nin	In	In	In	In	In	In
10	CYP_3A4 Substrate	Sub	W. Sub	W. Sub	Sub	W. Sub	W. Sub	W. Sub	Sub	Sub	Sub
11	Pgp_Inhibition[f]	NIn	NIn	NIn	Nin	NIn	In	In	NIn	In	In

(Fu -Fucoidan; Ag -Agar; Ga-Galactan; Al-Alginate; La-Laminarin; Xy-Xylan; Ma-Mannan; λ – Ca- λ Carrageenan; K Ca-K-Carrageenan; Po-Porphyran; In – Inhibitor; NIn– Non-Inhibitor; Sub- Substrate; W. Sub- Weak substrate)

[a] Blood–brain barrier (More than 1 – CNS active compound; Less than 1 CNS inactive compound) [b]HIA (0-20% - Poor absorption; 20-70% - Moderate absorption; 70-100% - Higher absorption) [c] Plasma protein Binding (%) (> 90 % , strongly bounded; <90 % weakly bounded) [d]Caco2 permeability (<4 , less ; 4-70, Moderate; >70, Higher)[e]CYP2D6 Non inhibitor-Accepted; CYP2D6 Non inhibitor- Rejected [f]P-gp- Inhibition - Non inhibitor – Rejected; P-gp- Inhibition -Inhibitor – Accepted

Table 9 — Toxicity profiling of macroalgal sulphated polysaccharides using protoxtool (A- Active; IA -Inactive)

S. No	Polysaccharides	Hepatotoxicity	Carcinogenicity	Immunotoxicity	Mutagenicity	Cytotoxicity	LD_{50} (mg/kg)	Class of toxicity
1	Fucoidan	IA	IA	IA	A	IA	1820	4
2	Agar	IA	IA	A	IA	IA	51	3
3	Galactan	IA	IA	IA	IA	IA	51	3
4	Alginate	IA	IA	IA	IA	IA	90	3
5	Laminarin	IA	IA	IA	IA	IA	23000	6
6	Xylan	IA	IA	IA	IA	IA	51	3
7	Lambda Carrageenan	IA	IA	IA	IA	IA	225	3
8	Mannan	IA	IA	IA	IA	IA	51	3
9	Kappa Carrageenan	IA	IA	IA	IA	IA	225	3
10	Porphyran	IA	IA	IA	IA	IA	225	3
11	Metformin (Control drug)	IA	IA	IA	IA	IA	680	4

Table 10 — Binding energy, Inhibition constant, Hydrogen & hydrophobic interactions of docking simulation of G6PC1 with metformin, fucoidan, and agarusingAuto dock

S. No	Protein	Ligand	Binding Energy (kJ mol-1)	Inhibition Constant (Ki)	No of H_2bonds	H_2bond atoms		Hydrophobic interactions
1	G6PC1	Metformin (Control drug)	-3.92	1.34mM	6	ALA37 ASP38 LEU39	GLY122 THR123 GLY118	NIL
2	G6PC1	Fucoidan	-4.32	680.08 µM	3	LYS76 HIS119 HIS119		GLU110 THR255
3	G6PC1	Agar	-3.06	5.75 mM	8	LEU3 ASP69 LYS76 GLU110	THR111 GLY112 GLY118 HIS119	LEU39

a crucial role in the G6Pase reaction. His residue in the G6Pase is phosphorylated during catalysis, leading to the formation of an enzyme-phosphate intermediate. H176 is the nucleophilic species that generates a phosphohistidine enzyme intermediate; R83 and R170 make H_2bonds with phosphate to stabilize the transition state, and H119 supplies the H^+ required to release the glucose molecule. When either H119 or H176 G6Pase is mutated, no enzyme phosphate intermediate is produced. For our docking studies, the amino acid residues R83, H119, R170, and H176 were chosen as active sites. Fucoidan exhibited the highest binding energies towards G6PC1 at -4.32 kJ/mol, comparable to metformin,

and formed 3 H2 bond interactions with L76, H119, and 2 hydrophobic interactions with E110 and T225. The agar exhibited a binding energy of -3.06 kJ/mol towards G6PC1, forming 8 hydrogen bond interactions with L39, D69, K76, E110, T111, G112, G118, and H119 and 1 hydrophobic interaction with L39. Fucoidan and agar formed H_2 bond interactions with G6PC1 target residue H119, rendering the enzyme inactive and generating no enzyme phosphate intermediate. The lack of significant binding energies of metformin towards G6PC1 suggests that there is no active site interaction taking place between this compound and G6PC1, while other 2 SPs are more selective towards G6PC1. A previous also study[37] reveals mutations in G6PC1, a hepatocyte-specific gene, cause extension of bleeding duration and unbalanced platelet aggregation, making it a potential target for diabetes control. Recent *in vivo* studies on mice reveal that deletion of G6PC2 affects β-cell metabolism, reducing fasting blood glucose levels without affecting fasting insulin levels[38]. Our study also supports previous studies indicating that fucoidan inhibit α-glucosidase and amylase activity, alters glucose retention into the circulation, and enhances insulin secretion *in vitro*[39]. Therefore, the SPs fucoidan and agar can be utilized as significant compounds against G6PC1 for the treatment of diabetes. Subsequently, Figures 5A-C shows the hydrogen and hydrophobic interactions of metformin, fucoidan, and agar with G6PC1, respectively.

Molecular dynamics (MD) simulations

GROMACS 5.0.4 was utilized for comparative MD simulations on the G6PC1 and G6PC1-fucoidan complex, with all simulations conducted for 50 ns timeframe. The RMSD measures the change in the protein backbone from its original configuration[40]. The G6PC1 RMSD for a 50 ns simulation was 0.450 nm,

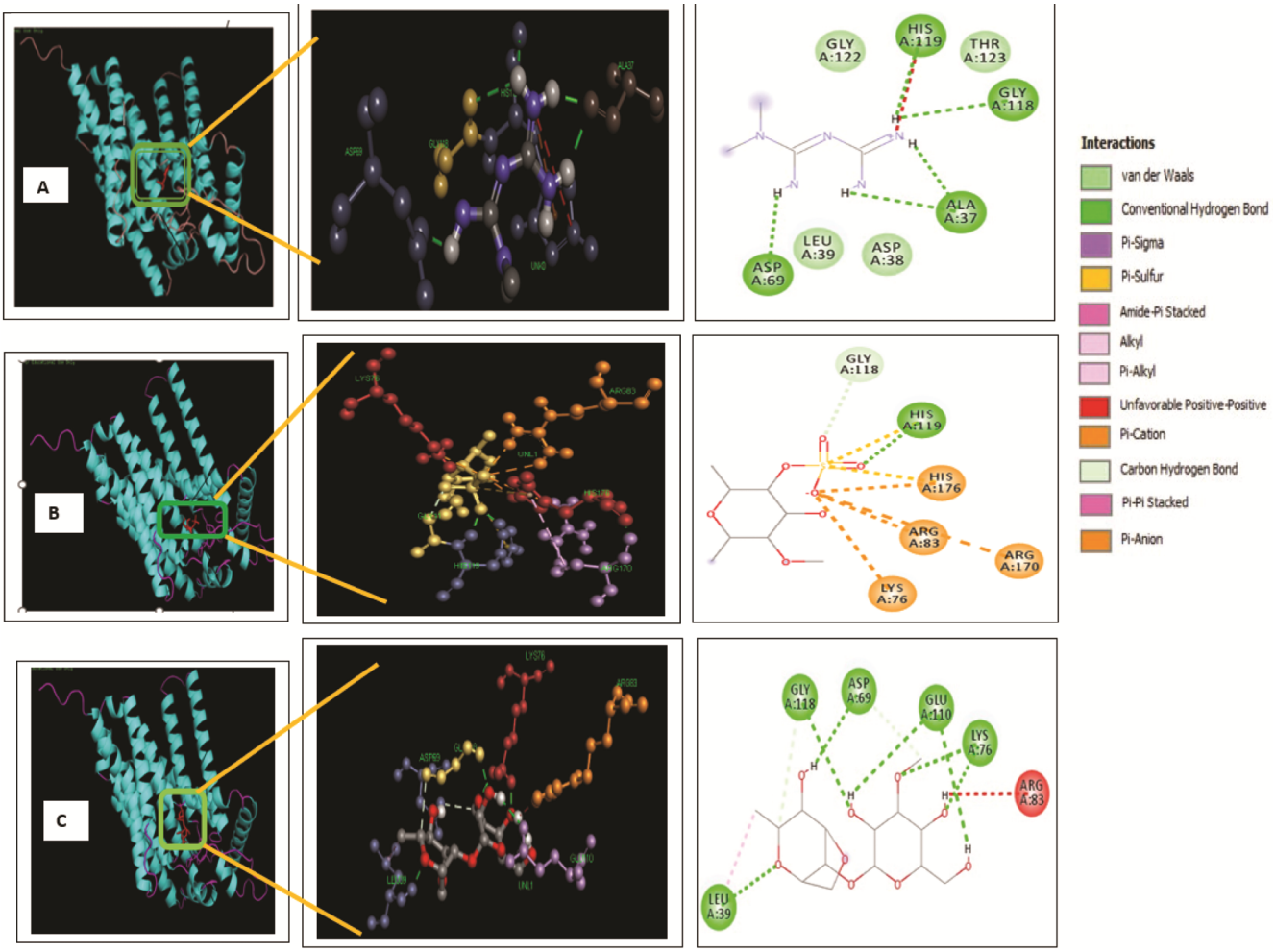

Fig. 5 — Docked complex, 3-D and 2-D molecular interaction of (A) Metformin; (B) Fucoidan; (C) and Agar with various G6PC1 amino acid residues

with oscillations between 0.35 nm and 0.55 nm. The G6PC1 exhibited stability between 12ns and 23ns, reaching a peak of 0.55 nm after 30 ns and remaining stable until 50 ns. The simulation of G6PC1-fucoidan reached stability at 20 ns with a 0.3 nm value and remained steady until the simulation's completion at 50 ns. The G6PC1 and G6PC1-fucoidan complex show a strong structural alignment, with both exhibiting a steady-state RMSD (Fig. 6). In our study, the RMSF profile identifies the flexible and rigid regions of the G6PC1 and the G6PC1-fucoidan complex.The RMSF analysis classified residues as mobile (0.20 nm and above), rigid (less than 0.20 nm), or extremely rigid (less than 0.1 nm). Based on our results, RMSF data of G6PC1 and G6PC1 fucoidan complexes showed minimal fluctuations (0.1-0.3 nm), indicating relative stability[41]. We also identified highly significant fluctuations in the range of 140 to 150 positioned residues in the G6PC1 and G6PC1 fucoidan complex's RMSF graph (Fig. 7). Rg allows one to analyze the changes in compactness of a ligand-protein complex[42]. The backbone atoms of the G6PC1 & G6PC1-fucoidan complex Rg were calculated to assess the system's local conformational stability (Fig. 8). All of the simulations of Rg graphs demonstrated that the structure's initial conformation

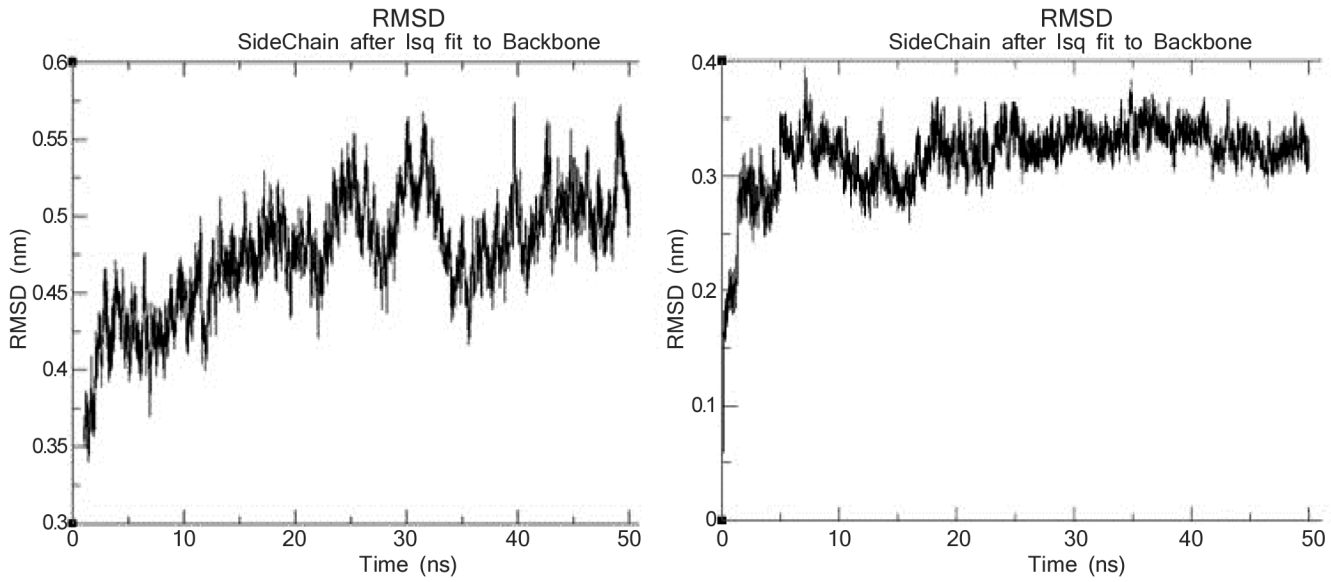

Fig. 6 — RMSD of G6PC1(a) & G6PC1-Fucoidan complex (b) using XM grace tool

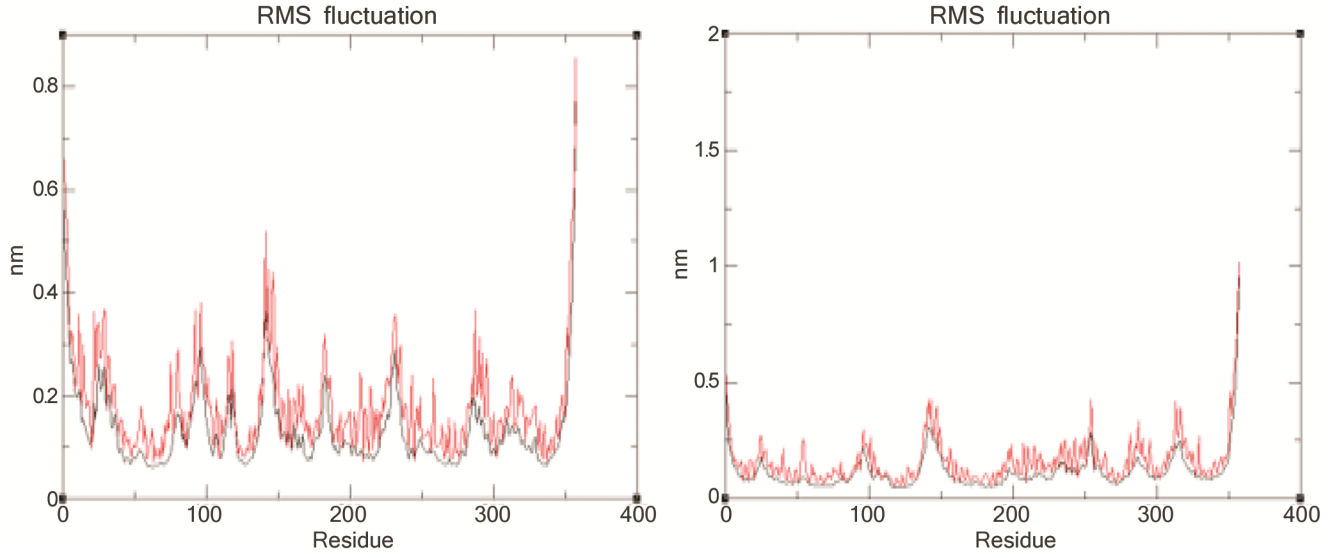

Fig. 7 — RMSF of G6PC1 & G6PC1-Fucoidan complex using XM grace tool

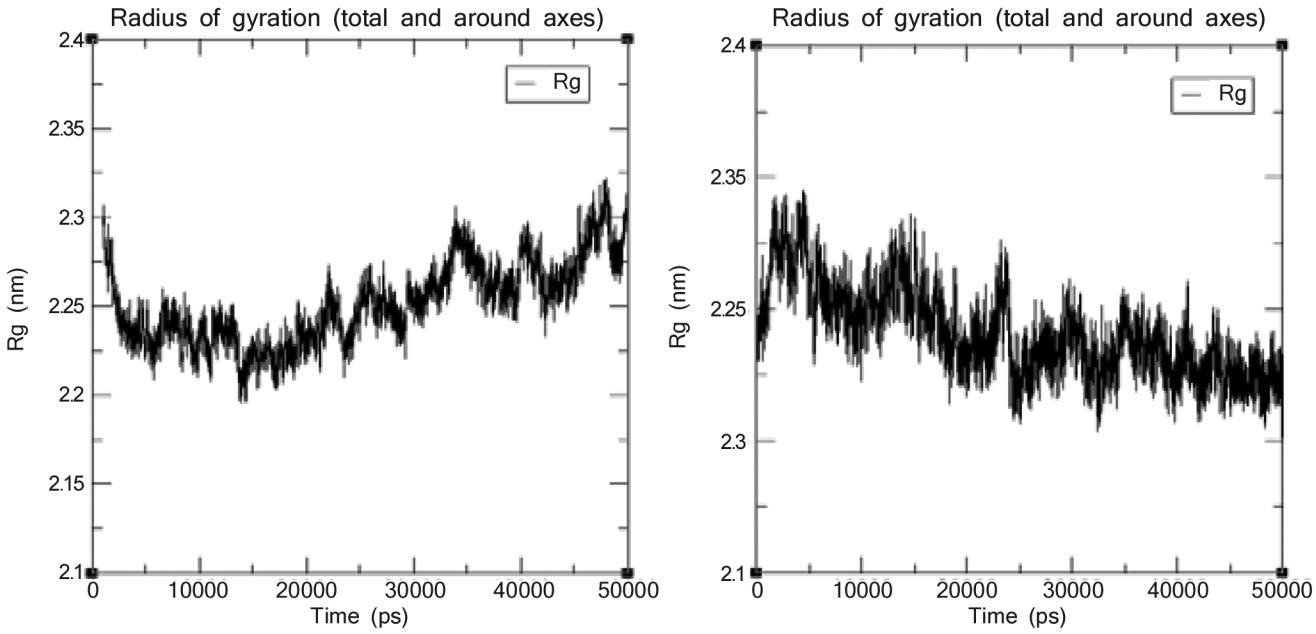

Fig. 8 — Radius of gyration of G6PC1 & G6PC1- fucoidan complex using XM grace tool

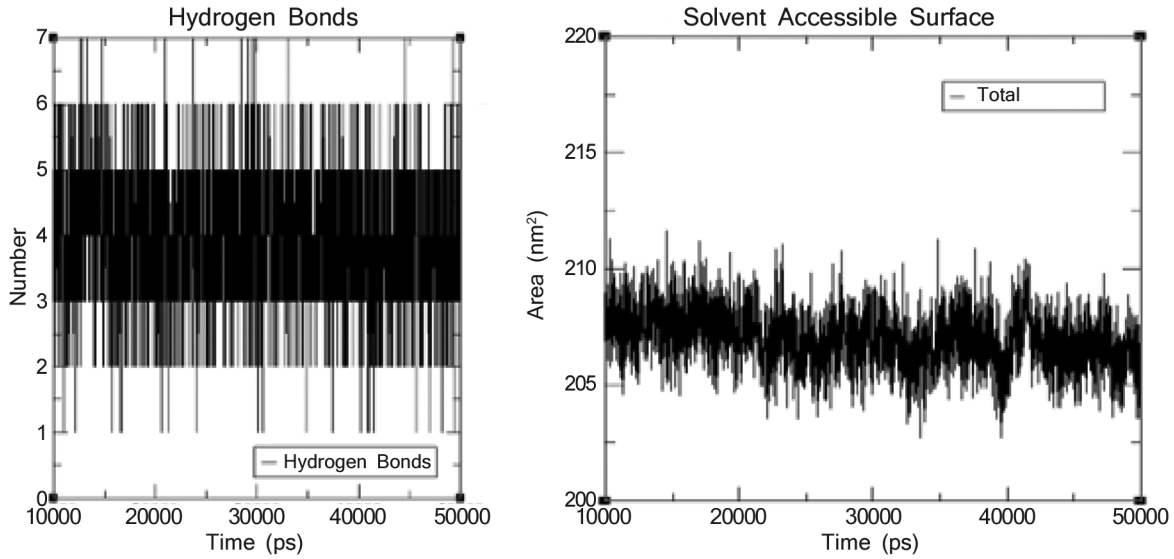

Fig. 9 — Hydrogen bonds and SASA of G6PC1-fucoidan complex using XM grace tool

was open, with the active site residues accessible to the solvent and the cavity of the active site exposed to allow the drug to bind. The Rg value in the G6PC1-fucoidan simulation was 2.3 nm at 0 ns, gradually decreasing to ~2.28 nm at 50 ns, maintaining an average value of around 2.28 nm. The active site pocket remains closed and unavailable until 50 ns. The Rg of G6PC1-fucoidan was reduced, suggesting that it has maintained a compact structure. The H_2 bond is crucial for enzyme-substrate binding, drug specificity, metabolism, and catalysis[43]. The simulation results indicate that the G6PC1-fucoidan complex maintains 2-6 H_2 bonds, indicating that fucoidan firmly binds to the G6PC1 active site. The stability and kinetics of protein folding were determined through a Solvent-accessible Surface Area (SASA) analysis. The G6PC1-fucoidan complex's SASA value during the 50ns simulation remained stable at 208 nm^2, indicating no structural changes in the protein (Fig. 9).

Conclusion

This study investigates the effect of marine algal SPs like fucoidan, agar, xylan, carrageenan, mannans, and 10 others on lowering G6PC1 activity using

computational methods. Drug-likeness, ADMET, and bioactivity characteristics have been tested for the 15 SPs, and it was found that fucoidan satisfied all the criteria. Furthermore, a protox toxicity test was determined to identify the toxicity levels of the selected SPs concerning a control drug, metformin. Sequence and structural analysis for the G6PC1were performed to find the protein homology and stability, respectively. Fucoidan also obeyed all the alternative drug likeliness rule-based filters and found more effective inhibitory activity against the G6PC1thanmetformin. Further MD simulations of RMSD, RMSF, and Rg for 50 ns revealed the G6PC1-fucoidan complex stability. Finally, *in silico* studies indicated that G6PC1 could be a possible pharmaceutical target for diabetes, and fucoidan could be an effective inhibitor of the G6PC1 enzyme. More *in vitro and in vivo* research is required to confirm SPs anti-diabetic inhibitory effects.

Acknowledgement

The authors express gratitude for Adam S. Ph.D. fellowship from AICTE ADF Scheme and the DBT-Govt. of India's Bioinformatics Infrastructure Facility at Anna University for computational support.

Conflicts of interest

All authors declare no conflicts of interest.

References

1 Bae JH, Han KD, Ko SH, Yang YS, Choi JH, Choi KM, Kwon HS & Won KC, Diabetes fact sheet in Korea 2021. *Diabetes Metab J*, 46 (2022) 1.

2 Sinclair M, Stein RA, Sheehan JH, Hawes EM, O'Brien RM, Tajkhorshid E & Claxton DP, Integrative analysis of pathogenic variants in glucose-6-phosphatase based on an AlphaFold 2 model. *PNAS Nexus*, 3 (2024) 36.

3 Abu Aqel Y, Alnesf A, Aigha II, Islam Z, Kolatkar PR, Teo A & Abdelalim EM, Glucokinase (GCK) in diabetes: from molecular mechanisms to disease pathogenesis. *Cell Mol Biol Lett*, 29 (2024) 120.

4 Rajas F, Gautier-Stein A & Mithieux G, Glucose-6-phosphate, a central hub for liver carbohydrate metabolism. *Metabolites*, 9 (2019) 282.

5 Matschinsky FM & Wilson DF, The central role of glucokinase in glucose homeostasis: a perspective 50 years after demonstrating the presence of the enzyme in islets of Langerhans. *Front Physiol*, 10 (2019) 148.

6 Pound LD, Oeser JK, O'Brien TP, Wang Y, Faulman CJ, Dadi PK, Jacobson DA, Hutton JC, McGuinness OP, Shiota M & O'Brien RM, G6PC2: a negative regulator of basal glucose-stimulated insulin secretion. *Diabetes*, 62 (2013) 1547.

7 Rui L, Energy metabolism in the liver. *Compr Physiol*, 4 (2014) 177.

8 Tan LS, Lau HH, Abdelalim EM, Khoo CM, O'Brien RM, Tai ES & Teo AK, The role of glucose-6-phosphatase activity in glucose homeostasis and its potential for diabetes therapy. *Trends Mol Med*, 31 (2025) 152.

9 Dhankhar S, Chauhan S, Mehta DK, Nitika, Saini K, Saini M, Das R, Gupta S & Gautam V, Novel targets for potential therapeutic use in diabetes mellitus. *Diabetol Metab Syndr*, 15 (2023) 1.

10 Citkowska A, Szekalska M & Winnicka K, Possibilities of fucoidan utilization in the development of pharmaceutical dosage forms. *Mar Drugs*, 17 (2019) 1.

11 The UniProt Consortium, UniProt: the universal protein knowledgebase in 2025. *Nucleic Acids Res*, 53 (2025) 609.

12 Gasteiger E, Hoogland C, Gattiker A, Duvaud SE, Wilkins MR, Appel RD & Bairoch A, Protein identification and analysis tools on the ExPASy server. *The Proteomics Protocols Handbook*, (2005) 571.

13 Altschul SF, Gish W, Miller W, Myers EW & Lipman DJ, Basic local alignment search tool. *J Mol Biol*, 215 (1990) 403.

14 Siever F & Higgins DG, Clustal Omega, accurate alignment of very large numbers of sequences. *Methods Mol Biol*, 1079 (2014) 105.

15 Jumper J, Evans R, Pritzel A, Green T, Figurnov M & Ronneberger O, Tunyasuvunakool K, Bates R, Žídek A, Potapenko A, Bridgland A, Meyer C, Kohl SAA, Ballard AJ, Cowie A, Romera-Paredes B, Nikolov S, Jain R, Adler J, Back T, Petersen S, Reiman D, Clancy E, Zielinski M, Steinegger M, Pacholska M, Berghammer T, Bodenstein S, Silver D, Vinyals O, Senior AW, Kavukcuoglu K, Kohli P & Hassabis D, Highly accurate protein structure prediction with AlphaFold. *Nature*, 596 (2021) 583.

16 Geourjon C & Deleage G, SOPMA: significant improvements in protein secondary structure prediction by consensus prediction from multiple alignments. *Comput Appl Biosci*, 11 (1995) 681.

17 Daina A, Michielin O & Zoete V, SwissADME: a free web tool to evaluate pharmacokinetics, drug-likeness and medicinal chemistry friendliness of small molecules. *Sci Rep*, 7 (2017) 42717.

18 Lee S, Lee IH, Kim HJ, Chang GS, Chung JE & No KT, The PreADME approach: web-based program for rapid prediction of physico-chemical, drug absorption and drug-like properties. *In: Euro QSAR 2002 - Designing Drugs and Crop Protectants: Processes, Problems and Solutions* (2002) 418.

19 Banerjee P, Eckert AO, Schrey AK & Preissner R, ProTox-II: a webserver for the prediction of toxicity of chemicals. *Nucleic Acids Res*, 46 (2018) W257.

20 Morris GM, Huey R, Lindstrom W, Sanner MF, Belew RK, Goodsell DS & Olson AJ, AutoDock4 and AutoDockTools4: automated docking with selective receptor flexibility. *J Comput Chem*, 30 (2009) 2785.

21 Abraham MJ, Murtola T, Schulz R, Pall S, Smith JC, Hess B & Lindahl E, GROMACS: high-performance molecular simulations through multi-level parallelism from laptops to supercomputers. *SoftX*, 1 (2015) 19.

22 Kaur G & Pati PK, *In silico* physicochemical characterization and topology analysis of respiratory burst oxidase homolog (Rboh) proteins from Arabidopsis and rice. *Bioinformation*, 14 (2018) 93.

23 Guruprasad K, Reddy BV & Pandit MW, Correlation between stability of a protein and its dipeptide composition: a novel approach for predicting *in vivo* stability of a protein from its primary sequence. *Protein Eng*, 4 (1990) 155.

24 Jaiswal A, Chhabra A, Malhotra U, Kohli S & Rani V, Comparative analysis of human matrix metalloproteinases: emerging therapeutic targets in diseases. *Bioinformation*, 6 (2011) 23.

25 Wilkins MR, Gasteiger E, Sanchez JC, Bairoch A & Hochstrasser DF, Two-dimensional gel electrophoresis for proteome projects: the effects of protein hydrophobicity and copy number. *Electrophoresis*, 19 (1998) 1501.

26 Dill KA, Dominant forces in protein folding. *Biochemistry*, 29 (1990) 7133.

27 Gill SC & von Hippel PH, Calculation of protein extinction coefficients from amino acid sequence data. *Anal Biochem*, 182 (1989) 319.

28 Mariani V, Biasini M, Barbato A & Schwede T, lDDT: a local superposition-free score for comparing protein structures and models using distance difference tests. *Bioinformatics*, 29 (2013) 2722.

29 Liu S, Tian F, Zhang C, Qiao Z & Zhao K, Genome-wide identification, phylogeny, and expression analysis of G6PC gene family in common carp, *Cyprinus carpio*. *Turk J Biochem*, 45 (2020) 205.

30 Cheng T, Zhao Y, Li X, Lin F, Xu Y, Zhang X, Li Y, Wang R & Lai L, Computation of octanol–water partition coefficients by guiding an additive model with knowledge. *J Chem Inf Model*, 47 (2007) 2140.

31 Khaled DM, Elshakre ME, Noamaan MA, Butt H, Abdel Fattah MM & Gaber DA, A computational QSAR, molecular docking, and *in vitro* cytotoxicity study of novel thiouracil-based drugs with anticancer activity against human-DNA topoisomerase II. *Int J Mol Sci*, 23 (2022) 11799.

32 Veber DF, Johnson SR, Cheng HY, Smith BR, Ward KW & Kopple KD, Molecular properties that influence the oral bioavailability of drug candidates. *J Med Chem*, 45 (2002) 2615.

33 Martin YC, A bioavailability score. *J Med Chem*, 48 (2005) 3164.

34 Buxton IO, Pharmacokinetics: the dynamics of drug absorption, distribution, metabolism, and elimination. *Goodman& Gilman's: The Pharmacological Basis of Therapeutics13e,* (2017).

35 Tornio A & Backman JT, Cytochrome P450 in pharmacogenetics: an update. *Adv Pharmacol*, 83 (2018) 3.

36 Ghosh A, Shieh JJ, Pan CJ, Sun MS & Chou JY, The catalytic center of glucose-6-phosphatase. HIS176 is the nucleophile forming the phosphohistidine-enzyme intermediate during catalysis. *J Biol Chem*, 277 (2002) 32815.

37 La Rose AM, Bazioti V, Hoogerland JA, Svendsen AF, Groenen AG, van Faassen M, Rutten MG, Kloosterhuis NJ, Dethmers-Ausema B, Nijland JH & Mithieux G, Hepatocyte-specific glucose-6-phosphatase deficiency disturbs platelet aggregation and decreases blood monocytes upon fasting-induced hypoglycemia. *Mol Metab*, 53 (2021) 101265.

38 Rahim M, Nakhe AY, Banerjee DR, Overway EM, Bosma KJ, Rosch JC, Oeser JK, Wang B, Lippmann ES, Jacobson DA & O'Brien RM, Glucose-6-phosphatase catalytic subunit 2 negatively regulates glucose oxidation and insulin secretion in pancreatic β-cells. *J Biol Chem*, 298 (2022) 101729.

39 Mabate B, Daub CD, Malgas S, Edkins AL & Pletschke BI, Fucoidan structure and its impact on glucose metabolism: implications for diabetes and cancer therapy. *Mar Drugs*, 19 (2021) 1.

40 Shukla R, Shukla H, Sonkar A, Pandey T & Tripathi T, Structure-based screening and molecular dynamics simulations offer novel natural compounds as potential inhibitors of *Mycobacterium tuberculosis* isocitrate lyase. *J Biomol Struct Dyn*, 3 (2018) 1.

41 Melk MM & El-Sayed AF, Phytochemical profiling, antiviral activities, molecular docking, and dynamic simulations of selected *Ruellia* species extracts. *Sci Rep*, 14 (2024) 15381.

42 Bhatt P, Joshi T, Bhatt K, Zhang W, Huang Y & Chen S, Binding interaction of glyphosate with glyphosate oxidoreductase and C-P lyase: molecular docking and molecular dynamics simulation studies. *J Hazard Mater*, 409 (2021) 124954.

43 Singh S, Kumar VB, Datta S, Wani AB, Dhanjal DS, Romero R & Singh J, Glyphosate uptake, translocation, resistance emergence in crops, analytical monitoring, toxicity, and degradation: a review. *Environ Chem Lett*, 18 (2020) 663.